Effect of Ultrasonic Process Parameter on Resistance and Plastic Deformation of the Aluminum Ribbon Bond on Molybdenum Layer

Sabarina Abdul Hamid
Renewable Energy Research Laboratory (RENERAL),
Electrical Engineering Section,
Universiti Kuala Lumpur
British Malaysian Institute,
Gombak 53100, Malaysia
sabarina@unikl.edu.my

Muhammad Nubli Zulkifli
Renewable Energy Research Laboratory (RENERAL),
Electrical Engineering Section,
Universiti Kuala Lumpur
British Malaysian Institute,
Gombak 53100, Malaysia
mnubliz@unikl.edu.my

Azman Jalar
Institute of Microengineering and Nanoelectronics and the Department of Applied Physics, Faculty of Science and Technology,
Universiti Kebangsaan Malaysia,
Bangi, Selangor 43600, Malaysia
azmn@ukm.edu.my

Maria Abu Bakar
Institute of Microengineering and Nanoelectronics,
Universiti Kebangsaan Malaysia,
Bangi, Selangor 43600, Malaysia
maria@ukm.edu.my

Wan_Nursheila Wan Jusoh
Fire Safety Research Cluster,
Aerospace Section,
Universiti Kuala Lumpur
Malaysian Institute of Aviation Technology 43800, Malaysia
wannursheila@unikl.edu.my

Hassan Basher
Renewable Energy Research Laboratory (RENERAL),
Electrical Engineering Section,
Universiti Kuala Lumpur
British Malaysian Institute,
Gombak 53100, Malaysia
yasr_yasr2001@yahoo.com

Michael Daenen
Faculty of Engineering Technology,
Hasselt University,
Campus Diepenbeek,
BE 3590 Diepenbeek, Belgium
michael.daenen@uhasselt.be

***Abstract*—The aim of this study is to evaluate the effect of process parameters on resistance and plastic deformation of ultrasonic aluminum ribbon bond on the molybdenum back contact layer of copper indium gallium selenide (CIGS) thin film photovoltaic (TFPV) solar panel. The aluminium ribbon was ultrasonically bonded on molybdenum with two process parameter settings with constant pressure and energy while varying the amplitude. The resistance measurement of the samples was conducted with two techniques which are the transmission line method (TLM) and micro-ohmmeter to evaluate the conductivity of the interconnection. Moreover, the plastic deformation of the aluminium bond from longitudinal and transverse cross-sections was examined by measuring the thickness of the aluminum bond. The resistance of the samples is directly proportional to the amplitude applied while the thickness of the aluminum for both longitudinal and transverse cross-sections is inversely proportional to the amplitude employed. By applying adequate pressure (3.5 bar) and energy (20 J), with the lower amplitude applied which is 7.7 µm, less plastic deformation occurs to the aluminum bond with lower resistance measured.**

Keywords—plastic deformation, ultrasonic bond, aluminium, molybdenum, resistance

I. INTRODUCTION

The interconnection strength of copper indium gallium selenide (CIGS) modules plays a crucial role in determining their long-term performance and durability. In particular, the bond strength between the aluminum (Al) ribbon and the molybdenum (Mo) layer, which serves as the back contact in CIGS solar cells, is of utmost importance. Ultrasonic bonding is one of the interconnection techniques applied which has the advantages of being cost-effective and less susceptible to thermo-mechanical stress, which is the leading cause of defects in CIGS TFPV solar panels [1]. The effect of process parameters and bonding strength of the ultrasonic bond was commonly evaluated by the contact resistance of the joint [2]–[4] and peel strength test [5], [6]. However, understanding the effect of process parameters on the resistance and deformation of the Al and Mo bond is critical for achieving reliable and efficient CIGS thin-film photovoltaics. The aim of this study is to evaluate the effect of ultrasonic process parameters on the physical properties of aluminium bonds on the molybdenum layer which are the resistance and plastic deformation. The study compares two methods of resistance measurement and measures the aluminum bond deformation by its thickness after the bonding process.

II. MATERIALS AND METHODS

A. Materials

The sample of this study is an aluminium ribbon of 2 mm width and 0.15 mm thick that ultrasonically bonded on thin film molybdenum (Mo) layer, which acts as back contact layer of CIGS thin film photovoltaic. The process of bonding was accomplished by using an ultrasonic Schunk DS-35 bonder with Mo layer thickness of 0.26 µm on top of the 3 mm thick glass substrate. Figure 1 shows a cross-sectional view of an ultrasonic Al bond, an Al ribbon, with the pressure

direction and amplitude applied during the ultrasonic bond process. Five bonds are applied on each ribbon and five Al ribbon lines are constructed on each sample.

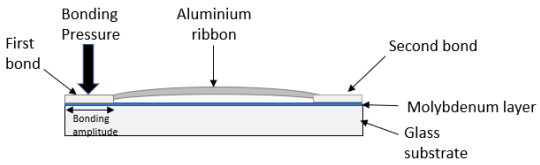

Fig. 1 Cross-sectional view of an ultrasonic Al bond

The aluminium ribbon was ultrasonically bonded on molybdenum with two process parameter settings with constant pressure and energy while varying values of amplitude as shown in Table 1. The sonotrode used in the ultrasonic bonder has dimensions of 5 × 3 mm².

TABLE 1: PROCESS PARAMETER OF ALUMINIUM ULTRASONIC BOND

Sample	Pressure (bar)	Maximum Energy (J)	Amplitude (µm)
A	3.5	20	9.1
B	3.5	20	7.7

B. Resistance measurement

Resistance measurement was conducted to evaluate the effect of process parameters on the sample's resistance. Resistance measurement was conducted using two techniques, the transmission line method (TLM) and the micro-ohmmeter. The TLM method measures the resistance between Al ribbon at different distances to evaluate the contact resistance between Al and Mo of the sample. While the micro-ohmmeter measures the resistance between bonds at constant distances of the Al ribbon.

Current (I) and voltage (V) were measured at room temperature in the dark room using the four-probe method. Fig. 2. shows the experimental setup of the TLM measurement where the current was measured by a precise SourceMeter 2400 current meter through four sequential contacts by maintaining a fixed voltage across those contacts. The aluminium ribbon bond on molybdenum with irregular spacing, D_i was arranged to form the TLM structure. The distance, Di between the ribbon was set at 3 mm, 6 mm, 10 mm, and 15 mm. The contact resistance was calculated from the intercept line of a straight-line graph of resistance versus distance [4], [7] .

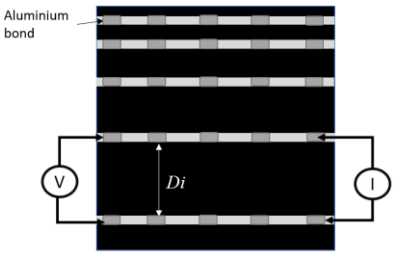

Fig. 2 TLM measurement experimental setup

Fig. 3 shows the experimental setup for micro-ohmmeter measurement where the kelvin probe from the micro-ohmmeter was connected at the center of the first and second bonds. The distance between the bonds is 10 mm, while the width and length of the bond are 2 mm and 3 mm respectively. The result of resistance was compiled and tabulated in a graph with calculated standard error to evaluate the accuracy of the measurement.

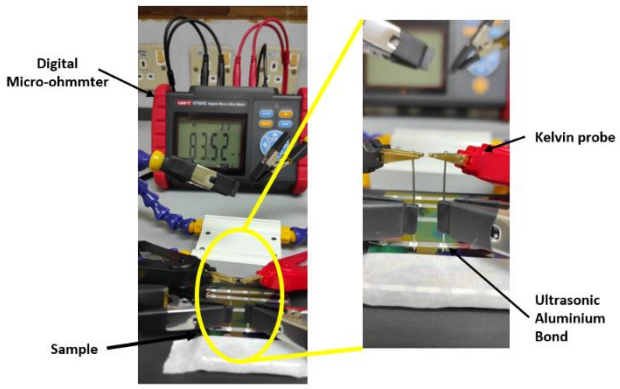

Fig. 3 Bonding resistance measurement using micro-ohmmeter at two bonds.

C. Sample preparation for cross-section evaluation

The cross-section of the bonded area was then cut into a longitudinal and transverse axis to evaluate the thickness and plastic deformation of the aluminium's ribbon bonded area. Fig. 4. shows the area of interest for sample preparation. Then, the samples were then cold mounted with resin, wet grinding progressively with finer abrasive grits papers of 280, 450, 800 and 1200. Finally the samples were polished with 6 µm, 3 µm, 1 µm and 0.25 µm diamond suspensions on silk cloth and final polishing with 0.05 µm alumina to reveal the cross-section image of aluminium bond.

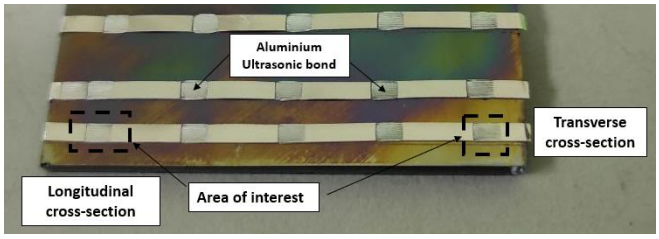

Fig. 4 Area of cutting for cross-section evaluation.

Cross-section images were captured with an AS Optic microscope 6.3MP Sony Exmor CMOS Sensor digital camera to allow accurate evaluation of the samples. In order to evaluate the deformation of aluminium after bonding, the image processing program called ImageJ software was used

to measure the average thickness of the aluminium bond [8]. The aluminium thickness is equal to the area divided by the length of the aluminium as shown in Fig. 5. The average thickness of the aluminium bond was calculated to evaluate the effect of process parameters on the thickness of the aluminium that will affect the conductivity of the interconnection. The thickness of the aluminium was compared to the resistance value obtained by both techniques.

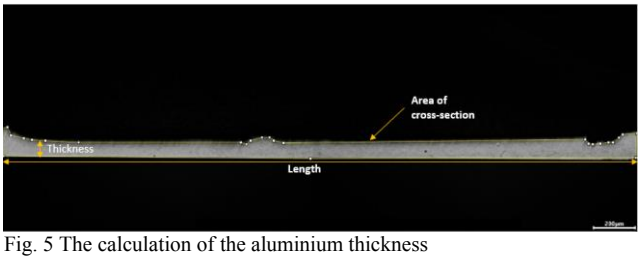

Fig. 5 The calculation of the aluminium thickness

III. RESULT AND DISCUSSION

A. Resistance of the sample

The average resistance of TLM and micro-ohmmeter technique was tabulated for samples A and B in Fig. 6 where sample B with low amplitude applied shows low resistance value for both TLM (8.25 mΩ) and micro-ohmmeter (111.15 mΩ) technique. The low resistance indicates a better intimate contact area between aluminum and molybdenum and improves the conductivity of the interconnection [9].

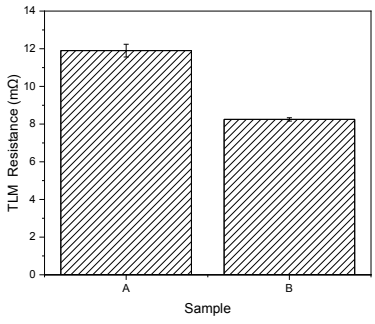

(a)

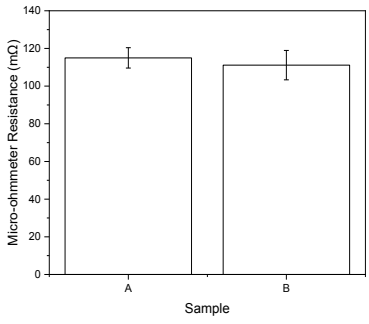

(b)

Fig. 6. Variation resistance of sample (a) TLM and (b) Micro-ohmmeter

The resistivity of both techniques was calculated and presented in Table 2. A directly proportional between the resistance values and the ultrasonic amplitude was observed in both techniques. Nevertheless, the differences between the two techniques were 1-fold. This is due to the type of probe and the accuracy of the equipment applied. The four-point probe used for TLM measurement has the accuracy and resolution of the current meter of 0.012% and 6½-digit resolution while the micro-ohmmeter was applied with a kelvin probe of +0.1% accuracy and 1μΩ resolution.

TABLE 2: VARIATION RESISTIVITY OF TLM AND MICRO-OHMMETER TECHNIQUE

Sample	TLM Contact Resistivity,ρc (mΩcm²)	Micro-ohmmeter Resistivity,ρ (μΩcm)
A	3.57	0.35
B	2.48	0.33

B. The thickness of the Aluminium Ribbon Bond

Fig. 7 and Fig. 8 show the optical microscope image of the aluminium bond in longitudinal and transverse cross-sections. The plastic deformation of the bond can be evaluated by measuring the thickness of the aluminium bond. The intense ultrasonic vibration will increase the slip and plastic deformation which then formed the bond [10]. The variation in thickness shows the plastic deformation process that takes place during the bonding process.

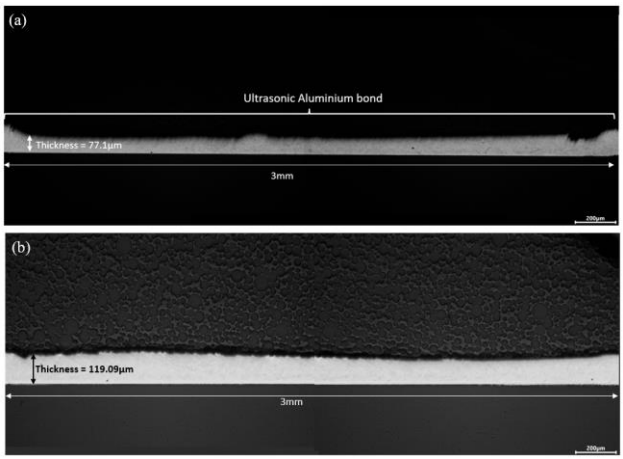

Fig. 7. The optical image of the aluminium bond in longitudinal cross-section (a) high amplitude (9.1μm) and (b) low amplitude (7.7μm)

The longitudinal and transverse cross-section images of sample A shown in Fig 7(a) and Fig 8(a) reveals that the plastic deformation at the peak and valley was more consistent than sample B in Fig. 7(b) and Fig. 8(b). This is due to the combination of sonotrode vibration and clamping force action that effect the wear behavior of the ultrasonic bond [11]. Mechanical interlocking is one of the most important factors in enhancing joint strength. The deformation and mechanical interlocking along the interface were the primary causes of joint formation [12], [13].

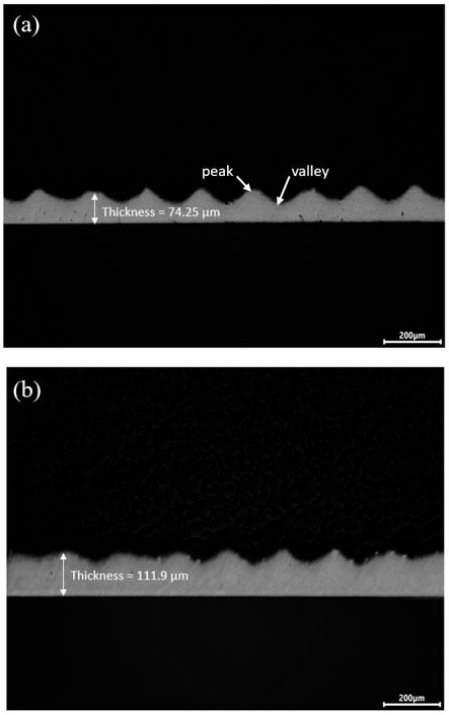

Fig. 9. The thickness of aluminium bond in transverse cross-section (a) high amplitude (9.1µm) and (b) low amplitude (7.7µm)

Applying the associated pressure and amplitude during the bonding process can enhance the bonding strength [5]. Vibration amplitude increases the frictional generation at the interface rapidly. When the ultrasonic bonding process is performed at a higher amplitude, extensive heat can be generated and non-uniform bonds can occur [3], [5]. However, detailed investigation by microstructure analysis through scanning electron microscope (SEM) is to be performed to investigate the existence of intermetallic compound (IMC) in between the interface of Al-Mo.

Fig. 10 shows the variation of aluminium thickness for longitudinal and transverse cross-sections. The thickness for sample A was 77.1 µm while sample B was 119.09 µm. The thickness of the transverse was slightly lower than the longitudinal cross-section of both samples. It is shown that the aluminium thickness is directly proportional to the ultrasonic amplitude applied for both longitudinal and transverse cross-sections. However, the cross-section thickness is inversely proportional to the resistance. Fig. 5 indicates that sample B with higher thickness has low resistance for both TLM and micro-ohmmeter techniques.

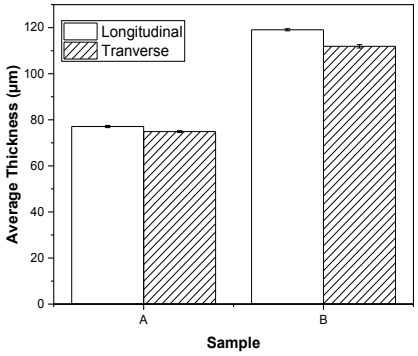

Fig. 10. The thickness variation of the longitudinal and transverse cross-section

The thickness of the peak and valley of the transverse cross-section sample was measured to evaluate the consistency of deformation after the bonding process with different amplitudes applied. As shown in Fig. 11, the thickness of the aluminium for the peak and valley indicates that at higher amplitude applied for Sample A, the more consistent plastic deformation with 100.03 µm thickness at the peak and 59.71 µm at the valley.

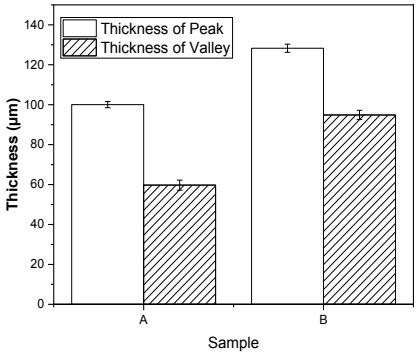

Fig. 11. The peak and valley thickness variation of the transverse cross-section

IV. CONCLUSIONS

The effect of process parameters of ultrasonic bond on the resistance of the samples as well as the plastic deformation by evaluating the thickness of the aluminium bond was studied.

The results show that the amplitude of the ultrasonic parameter is directly proportional to the resistance. The low resistance attained with a lower amplitude applied indicates better intimate contact between aluminum and molybdenum. Furthermore, the plastic deformation of the bond was evaluated by comparing the thickness of the sample for both longitudinal and transverse cross-sections which indicated that low aluminum thickness at higher amplitude applied. This indicates that the higher amplitude applied will affect more plastic deformation. By applying adequate bonding pressure of 3.5 bar and energy of 20 J, with the lower amplitude applied which is 7.7 µm is desirable, where low resistance was obtained with less plastic deformation of the aluminum bond.

ACKNOWLEDGMENT

This work was sponsored by the Ministry of Higher Education of Malaysia under the Fundamental Research Grant Scheme (FRGS/1/ 2020/TKO/UNIKL/02/10).

REFERENCES

[1] M. T. Zarmai, N. N. Ekere, C. F. Oduoza, and E. H. Amalu, "A review of interconnection technologies for improved crystalline silicon solar cell photovoltaic module assembly," *Appl Energy*, vol. 154, pp. 173–182, Sep. 2015, doi: 10.1016/j.apenergy.2015.04.120.

[2] M. Heimann *et al.*, "Ultrasonic bonding of aluminum ribbons to interconnect high-efficiency crystalline-silicon solar cells," in *Energy Procedia*, Elsevier Ltd, 2012, pp. 670–675. doi: 10.1016/j.egypro.2012.07.127.

[3] T. Xu, O. Valentin, and C. Luechinger, "Reliable metallic tape connection on CIGS solar cells by ultrasonic bonding," in *Thin Film Solar Technology II*, SPIE, Aug. 2010, p. 77710R. doi: 10.1117/12.860962.

[4] H. Basher, M. N. Zulkifli, A. Jalar, and M. Daenen, "Effect of Ultrasonic Bonding Parameters on the Contact Resistance and Bondability Performances of CIGS Thin Film Photovoltaic Solar Panel," *IEEE J Photovolt*, pp. 1–9, 2021, doi: 10.1109/JPHOTOV.2020.3047295.

[5] S. K. Patel, H. K. Dave, and H. V. Patel, "Ultrasonic Welding of Molybdenum Using Aluminium Interlayer," in *Advances in Additive Manufacturing and Joining*, Springer Nature Singapore Pte Ltd. 2020, 2020, pp. 669–677. doi: 10.1007/978-981-32-9433-2_59.

[6] S. Mostafavi and B. Markert, "Ultrasonic weld strength and weld microstructure characteristics in multi-strand aluminum cables (EN AW-1370) – Effect of process parameters," *J Manuf Process*, vol. 57, no. July, pp. 893–904, 2020, doi: 10.1016/j.jmapro.2020.07.054.

[7] S. Guo, G. Gregory, A. M. Gabor, W. V. Schoenfeld, and K. O. Davis, "Detailed investigation of TLM contact resistance measurements on crystalline silicon solar cells," *Solar Energy*, vol. 151, pp. 163–172, 2017, doi: 10.1016/j.solener.2017.05.015.

[8] N. Z. M. Mokhtar *et al.*, "Effect of electromigration and thermal ageing on the tin whiskers' formation in thin sn–0.7cu–0.05ga lead (pb)-free solder joints," *Coatings*, vol. 11, no. 8, 2021, doi: 10.3390/coatings11080935.

[9] H. Basher, M. N. Zulkifli, A. Jalar, and M. Daenen, "Temperature Cycling Test on Ultrasonic Aluminum Bonds and Conductive Adhesive of Copper Indium Photovoltaic Solar Panel," *IEEE J Photovolt*, pp. 1–10, 2022.

[10] Y. Long, J. Twiefel, and J. Wallaschek, "A review on the mechanisms of ultrasonic wedge-wedge bonding," *J Mater Process Technol*, vol. 245, pp. 241–258, Jul. 2017, doi: 10.1016/j.jmatprotec.2017.02.012.

[11] Z. L. Ni, J. J. Yang, and F. X. Ye, "Microstructure and mechanical properties of copper to nickel ultrasonic spot welds," *Materials Science and Engineering A*, vol. 796, no. February, 2020, doi: 10.1016/j.msea.2020.140207.

[12] B. Sanga, R. Wattal, and D. S. Nagesh, "Mechanism of joint formation and characteristics of interface in ultrasonic welding: Literature review," *Periodicals of Engineering and Natural Sciences*, vol. 6, no. 1, pp. 107–119, 2018, doi: 10.21533/pen.v6i1.158.

[13] Z. Zhang, K. Wang, J. Li, Q. Yu, and W. Cai, "Investigation of Interfacial Layer for Ultrasonic Spot Welded Aluminum to Copper Joints," *Sci Rep*, vol. 7, no. 1, pp. 1–6, 2017, doi: 10.1038/s41598-017-12164-2.